TECHNICAL ASPECTS OF HUYGENS SSP PENETROMETER DESIGN

Z.J. Krysiński,[*] J.C. Zarnecki, M.R. Leese,[†] R. D. Lorenz[‡]
D. J. Parker, M. Bannister, M. Sandford, J. Delderfield, P. Daniell, H. Jolly[§]

Abstract

This paper describes several technical issues related to the control system of the penetrometer ACC–E in the *Huygens Probe*, SSP package, employed in the *Cassini* mission. First, the piezoelectric transducer, made of the ceramic PZT 5–A, and its performance as a charge generator is described. Subsequently various signal conditioning requirements, to ensure the goals of the control, are discussed. They include: pseudo-logarithmic compression of signals, trigger functions, RMS signal generation, control of the trigger threshold level for proper touchdown detection, FIFO data buffer, and onboard in–flight test facilities. Several schemes and pre–flight test results are appended.

1 Introduction

The ESA *Huygens Probe* is part of the joint NASA, ESA & ASI mission *Cassini*. The goal of the mission was to reach the unknown surface of Titan. The probe had to survive at least two hours descent, land softly on the liquid or solid surface and, if it survived impact, to continue transmitting data for at least three minutes thereafter.

A number of sensors, comprising the *Surface Science Package* (SSP), were implemented to measure physical properties of the surface and to monitor the operating history. Among them were piezoelectric sensors and their conditioning subsystems. One of these, the external force sensor ACC–E, was mounted on a short pylon to measure the penetration force at impact. It provided information concerning the characteristics of the ground, in particular for impact on hard, solid surfaces, which might cause the thin fore–dome of the probe to deform. The SSP electronic system was designed to provide more control functions to support: ACC–I (an internal accelerometer), DEN (densitometer), THP

* *Space Research Center, Pol.Ac.Sci. / Rutherford Appleton Lab, Didcot, Chilton, UK*
† *PSSRI, The Open University, UK*
‡ *Lunar and Planetary Lab, University of Arizona*
§ *Members of SSP team*

(thermal properties instrument), TIL (tilt sensor) and PER (permittivity sensor), which was combined with CON (conductivity sensor). ACC–I was attached to the internal SSP box and responded to the deceleration of the probe platform. The purpose was to indicate a sharp deceleration at impact, as expected specifically for soft solid and for liquid impacts. These events would last longer than hard impacts, and thus ACC–I could be sampled at 0.5 kHz, that is, lower than ACC–E, which was sampled at 10 kHz. A hard touchdown on a solid surface was to be detected by the accelerometer ACC–E. Therefore, the accelerometer ACC–E had to acquire data faster than ACC–I.

The fundamental scientific goals of investigating Titan's surface were defined before the *Huygens Probe* was accepted, that is in the early 1990's. Proper reports are published in Zarnecki et al. (1991) and Zarnecki (1992). This paper deals only with technical and functional issues related to the electronic systems. Results obtained from the mission are reported in Owen (2005) and Zarnecki et al. (2005). More information can be found in Lorenz et al. (1994) and Lorenz et al. (2008).

2 Force or stress transducer

One of the penetrometer force transducer's purposes was determining the *Huygens Probe's* response to the surface impact. Considering a number of factors during the probe's parachute landing on a possibly solid surface, the penetrometer measurement range was designed to be from zero to 1000 N. The upper limit of 2000 N was considered as the destruction level, where the sensor or its fixture is expected to fail. The resolution for this measurement is a few [N]. The *Huygens Probe's* force or stress transducer acts electrically as a charge generator. It is known that some crystals, when deformed, generate an electrical charge (Encyclopaedia Britannica, 1977). Such crystals, which acquire charge when compressed, twisted or otherwise distorted, are called *piezoelectric crystals*. The same behaviour is seen in piezoelectric ceramic, for example the PZT ceramic (piezoelectric zirconate titanate), which was used in the *Huygens* force transducer. The PZT–transducer is a ceramic resonator for elastic waves. It is available in the shape of bars, discs, or rings. They can be easily adapted to lightweight constructions in order to provide a convenient charge–generating transducer. For the *Huygens* probe, the aim was to sense the impact force during the probe's touchdown. The transducer was designed as a ring sensor, compressed between a dome–shaped front piece and the pylon protruding from the front of the *Huygens Probe*. The length of the pylon was only a few cm. There were also other sensors working as accelerometers located inside the probe compartment, which provided more information on the behaviour of the probe structure, on tilting, and on the movements and vibrations during the descent and the impact phase.

The scientific purpose for ACC–E was to investigate the ground strength at the impact point. However, in addition to the impact force the PZT–sensor is also sensitive to the stress in the holding structure, which is highly dependent on temperature. Finally the impact force has to be separated from the temperature–induced stress. The descent and touchdown phase is influenced by numerous temperature trends, drifts and shock events. Finally the impact force must be separated from the various temperature–induced effects. There was the fear that temperature discontinuities during descent could be mis–interpreted as the impact–induced temperature shock. The thermal protection shell of the probe warms up to 900°C during the descent phase, but the PZT–sensor should not feel more then $250-300$°C in any case, because PZT–5A loses sensing capabilities at the Curie point 350°C. However, it was predicted that the temperature increase upon impact should remain much below the Curie point. Another fear regarding temperature shocks is related to pyro–electric effects proper to this kind of sensors, which are associated with a fast or abrupt increase of the ambient temperature. These pyro–electric effects may jeopardize the sensor by destroying the front–end electronics by an excessive voltage at the sensitive input, or at least by saturating an amplifier and thus creating a critical risk for the entire action. The protection was undertaken externally by the thermal shell, and internally, in electronics, by the entire complex of conditioning the trigger signal. Nevertheless, housekeeping measurements of the local ambient temperature are certainly helpful for analysing the accelerometer performance. In particular the apex point temperature can provide useful information for assessing how the PZT reacts thermally on the impact.

3 Transducer performance

The output parameters of the PZT device depend on its chemical structure, on the shape of the resonator, and on the pattern of the terminal electrodes. The FM (Flight Model) transducer model was a flat ring, made of PZT–5A ceramics and operating in the mode of a thickness expander (Lorenz et al., 1994). The ring was about 1 mm thick. The outside diameter is ca. 14 mm and the inside diameter 7 mm. Typically, the quality factor is $Q = 500 - 5000$. One side of the transducer is completely coated with the ground electrode, while the other side is covered by two round electrodes. The first round electrode is the sensing electrode. The second one was used as a stimulation source for testing the entire system including the transducer in flight. The dependence of the relative dielectric constant of the PZT–5A ceramic on temperature is shown in Figure 1.

The transducer, assembled in a mechanical structure, was very sensitive to possible strains and forces from the fixing system. The electronic system had to manage effects of non–repeatable assembly causing modifications of sensitivity and shifts of eigen–mode frequencies. The calibration and tuning had to allow sufficient margins.

4 Transducer connection

The transducer was connected to the pre–amplifier by means of a pair of coaxial cables. The cable length varies with stress and temperature (the so–called tribo–electric effect) and with the specimen, depending on design and manufacturing. Moreover, a voltage amplifier is sensitive to the cable length, and therefore a charge amplifier was applied. The design of the sensor assembly minimizes tribo–electric effects by burying the cables in a stiff foam filling. The effects were monitored by the level of the background noise produced by the system under vibrations. The input was protected by a charge attenuator preserving the desired dynamic range of the transducer. The force transducer element

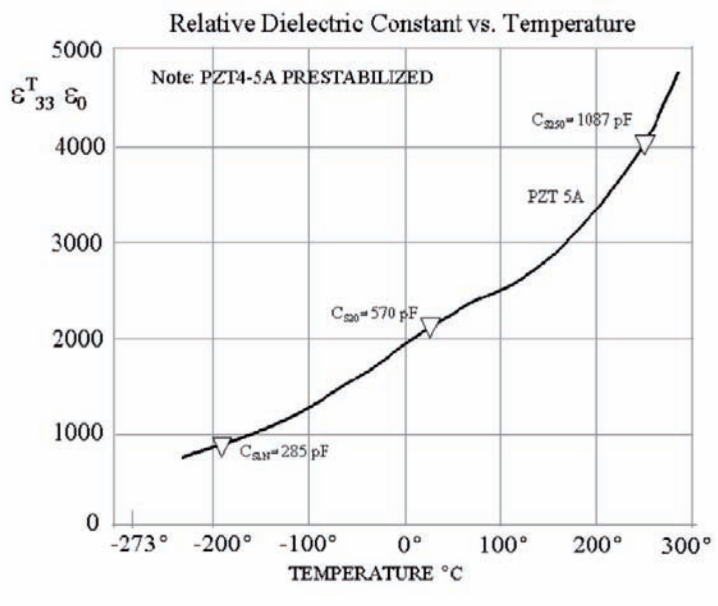

Figure 1: Plot of the relative dielectric constant of the PZT–5A ceramic vrsus temperature. It shows dielectric changes versus temperature. This plot shows the safe operating range. Values beyond 280°C, are close to the Curie temperature, 350°C, and should be avoided. The capacity values C_{SLN}, C_{S20} and C_{S250} represent the employed transducer in three characteristic temperature ranges possible in the mission. The left one is for LN_2 (liquid nitrogen), the middle one is room temperature in tests, and the right one (+250°C) is the maximum allowable operation temperature.

is shown in Figure 2 and described in Lorenz et al. (1994). Three separate cables were used to connect the force sensor and the conditioning electronics. The first two is a shielded pair of wires. The third one is a section of the coaxial cable. The length of the cables is about 1 m. The specific capacitance C (conductor–to–conductor) is $\approx$ 60 pF/m and C (conductor–to–shield) is $\approx$ 100 pF/m. These capacitances connect the input and stimulation signals by means of the wires and the coaxial line, respectively.

5 Front–end electronics

5.1 Charge pre–amplifier

A pre–amplifier was used for the first front–end conditioning of the transducer signal. It was a charge amplifier, instead of the usually employed voltage amplifier. The pre–amplifier supplies the output voltage proportional to the charge obtained from the transducer. The equivalent circuit of the front–end electronics, including transducer, charge

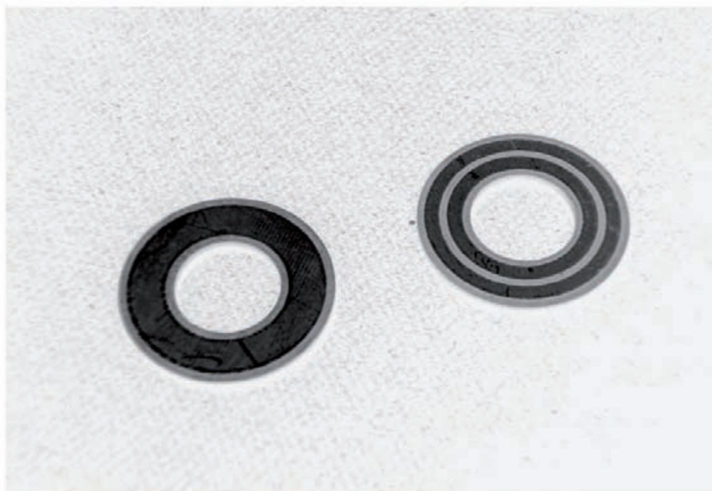

Figure 2: The PZT electrode layout for the force transducer. The outer diameter of the circle is 14 mm, while the inside is 7 mm. The specimen side (left), is coated with the ground electrode, while the other side (right) is covered by two concentric round electrodes, internal and external. The external electrode is predicted for instrumental and touch down sensing, the internal one is for monitoring the entire system, including the transducer. The in–flight test required a possibility of stimulating the transducer remotely, in order to examine the health of the instrument. For this purpose stimulus generated by the control system is applied to the internal electrode.

divider and connecting cable is shown in Figure 3.

The pre-amplifier closed loop gain is determined by R_F and C_F. The input resistance values are: R_{P+} , R_{P-} = 10 MΩ. The gain value is $A = -1$ V/V. The load resistance value is approximately $R_L \approx 10$ kΩ. The charge divider is to provide a charge protection of the pre–amplifier input. Suggested values for the front–end design were $C_1 = 9.4$ nF (to reduce the effective transducer output charge), and $C_2 = 390$ pF to tune the charge injected to the protected pre–amplifier input. C_S is the capacity representing the ring PZT–5A and electrodes; the measured values are: $C_{Stot} \approx 590pF$, $R_{Stot} \approx 293K$ whereby C_{Stot} comprises capacity of the transducer bulk material.

5.2 Noise conditioning

A physical stimulus of the transducer has a random nature due to fracture of the medium and the impact. The response is complex and random in magnitude and spectral components. The care about intrinsic noises of the system is motivated differently than in linear systems. Essentially, the front–end electronics serves nonlinear and large signal operation. It has to be reasonably robust, but also highly sensitive to small stimulating forces, both fast and slow ones; and it also has to transfer large magnitude components,

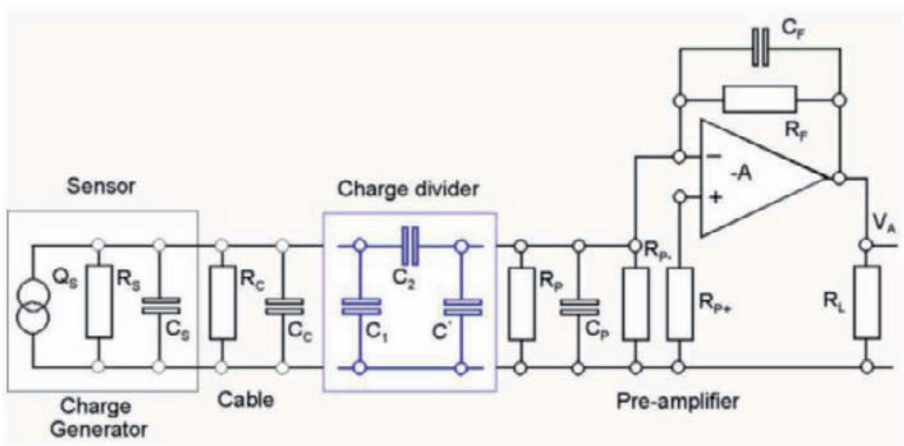

Figure 3: Equivalent circuit of the force sensor, the charge divider and the charge amplifier. The circuit comprises the following elements:
- Q_S *is the perfect charge source* ($C_Q = 570pF_{300K}, C_Q = 285pF_{77K}$, *manufacturer data);*
- C_S *is the capacity representing the ring PZT-5A and electrodes;*
- R_S *is the PZT internal leak resistance, negligible in practice;*
- R_C *is the specific cable resistance (estimated as* $R_C > 10^{15}\Omega/m$*);*
- C_C *is the specific cable capacitance (specified above);*
- R_{P-} *is the pre-amplifier inverting input resistance* ($10M\Omega_{diff}, 200G\Omega_{common}$)
- C_P *is the pre-amplifier inverting input capacitance, (3.2pF);*
- *A is the open loop gain (A>3000 V/mV), dependent on the load resistance* R_L*;*
- R_F *is the feedback resistance (10MΩ);*
- C_F *is the feedback capacitance (3nF);*
- C_1 *is the charge divider shunting capacitance (9.4nF)*
- C_2 *is the series capacitance (390pF)* R_{P+} *is the pre-amplifier non-inverting resistance (10MΩ).*

avoiding saturation of the signal system. The concern about noise is at least double–fold. On one hand, fast noise signals can provide sufficiently large energy to release the trigger, freezing the process of gathering data in the FIFO data buffer. This false trigger could prevent the real touchdown from being measured. On the other hand, slow noise signals may create also a danger by changing the trigger level and thus modifying the trigger time. Slow noise may thus affect the length of the touchdown sequence saved after the trigger. The release time should be secure and resistant to any jitter.

There are several possible sources of noise in the system. Some noise may come with the power supply lines, some may be induced electromagnetically, some else is simply generated by solid state devices, passive components and the transducer itself. In general two types of noise are considerable: the shot noise related to the density of the conduction current, and the $1/f$ noise, proper to semiconductor elements. The $1/f$ noise pertains a random recombination of donor traps in solid state devices, especially on crystal (wafer) surfaces. This kind of noise may be also stimulated externally by hard radiation.

The signal system does not employ special means of noise reduction. It is a single channel chain, but not a balanced differential system, so the only means to control the contribution of the various noise sources is limiting the lower frequency limit (LFL) and the upper frequency limit (UFL) by simple filtering. A signal from the transducer is limited to the pass band, and sampled. Sampling brings also side effects of filtering. That part of the signal spectrum, which falls beyond the cutoff frequency, is determined by the sampling rate. It is sampled and then its high frequency contribution is back–converted to the pass band, producing an undesired distortion of the signal known as aliasing. To minimize the effect of aliasing, one needs not only to cut off the excessive part of the spectrum, but also to match the phase characteristics of filtering to the sampling rate and the phase characteristics of the system. This match is usually imperfect. A proper anti–aliasing filtering has been applied for the UFL side. From the LFL side, the low frequency noises have been limited by the feedback loop in the charge–amplifier, determined by the elements C_F, R_F (see Figure 3). The open loop gain of the charge amplifier is $A = 3 \times 10^6$ (according to the manufacturer data), what yields an LFL of about 0.002 Hz.

Externally, the charge amplifier is an unipolar passband amplifier with the bandwidth limited from the low and high sides. It truncates only the positive part of the waveform. Internally, it conducts the signal from DC. The transient characteristics of the amplifier is nonlinear. There are two nonlinear properties. The first one rejects one half of the waveform at the charge amplifier input. The second one avoids saturation by utilising a logarithmic amplifier as the second stage. The primary goal of the system is to produce a touchdown signal properly, so it is accepted that the recorded waveform is distorted. Its spectral content is still corresponding to the history of the impact and allows recognition of the ground surface properties. The touchdown signal is determined from the DC–like component. A sufficiently high rise corresponds to the energy of the waveform received, averaging with a defined time constant. The RMS value of the impact signal is determined. If it achieves, or crosses the threshold level, then the trigger must be released to freeze the contents of the data buffer. The FIFO data buffer is permanently filling with data until the trigger point. After trigger it contains 64 words corresponding to the pre–triggered state and 448 words post–trigger.

That way the data, believed to contain the record of the touchdown, are available for reading and further processing. However, the intrinsic noises can disturb this plan and in the worst case even produce a false trigger signal. Then the touchdown data could be missed. The purpose of employing the noise control is to improve the accuracy of the trigger. Trigger operation must be sure in the presence of noises, and determined by a proper definition of the threshold level. The threshold level is desirably set high, well above the level corresponding to the RMS contribution from the intrinsic noises. All relations between LFL, UFL, sampling, system non–linearity, noise level and the trigger threshold level are subject to tuning, trimming and adjusting on the base of the tests which had to be performed for each particular assembling of the transducer. Repeatability of the transducer mounting determined the success.

5.3 Dynamic conditioning

This nonlinear transient characteristic was required to make the system capable of detecting the touchdown under soft and hard impact conditions. The logarithm–like characteristic was desired to store the data gathered after the first touchdown. Keeping in mind the limited resources available to the electronics, a logarithmic type function was found to be most suitable to cover the expected range of possible responses. Using such an amplifier characteristics is a kind of compression, before it is sampled and converted to digital form. The compression affects the entire signal spectrum. An upper limit frequency (UFL) due to the sampling rate has been considered, and an anti–aliasing filtering has been introduced. The pseudo–log amplifier increases small signals and a suppresses large signals. After the pseudo–log conversion the signal is prepared for sampling. The signal is directed to an S/H sampler (sample and hold).

5.4 Upper limiting frequency filter

The anti–aliasing filter is put into the signal chain at the output of the pseudo–log converter. The sampling rate is 10 kHz and the resulting cutoff frequency is 5 kHz. The anti–aliasing filter is determined by the components shown in Figure 4. Its function is to match the phase transmission characteristics to the sampling rate, including the overall phase effect of the front-end conditioning. The UFL filter was trimmed and adjusted to minimize aliasing.

5.5 Analog–to–digital converter

The AD7821 (not shown here) is an 8 bit sampling AD converter with an overflow 9^{th} bit, which terminates the main analog track of the ACC–E electronic system. It operates with unipolar input in the full range of U_{IN} = 0 V to U_{IN} = 4.5 V. A high precision reference voltage U_{REF1} = 4.5 V supports digitalization performed by this converter. This reference element has an ageing rate of 25 ppm per 1000 hours. The logic outputs, are set as DB0 – DB7, corresponding to LSB (least significant bit) and MSB (most significant bit) respectively. The ADC logic outputs feed appropriately the logic inputs of the FIFO data buffer. Finally, the S/H function was decided (in 1992) to be added to the pre–flight version. Its mode was sampling and tracking and the applied sampling rate was 10 kHz.

The ACC–E ADC is one out of three ADC converters used in the SSP system. The other converters were: the 16–bit ADC dedicated to digitize the THP signals, referred to the reference source U_{REF2} = 4.5 V, and the 12–bit ADC, referred to the internal U_{REF} = 10 V. The 12–bit ADC performs digitalization of signals acquired by other following subsystems: ACC–I, PER/CON, TIL and DEN.

5.6 FIFO–buffer

The impact sensor data is stored in a FIFO data buffer at a rate of 10 kHz. When the system is active, the buffer is continuously filled up by the data stream. On touchdown

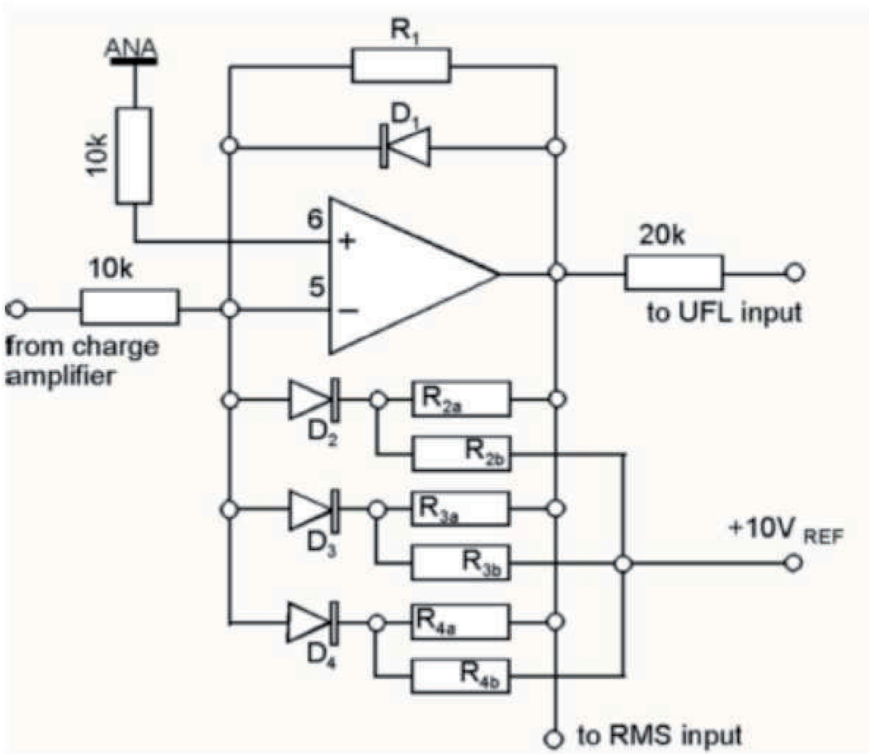

Figure 4: The inverting pseudo–log converters scheme. This circuit is forming the desired logarithmic characteristics by use of three voltage thresholds set by the diodes D_2, D_3 and D_4 and by selected pairs of resistors R_{2a}, R_{2b} and R_{3a}, R_{3b}, and R_{4a}, R_{4b}. Slopes of linear fragments of the characteristics are set by R_1 in relations with resistors mentioned above. The output voltage swing depends on the +10 V_{REF} and on the clamping diode D_1.

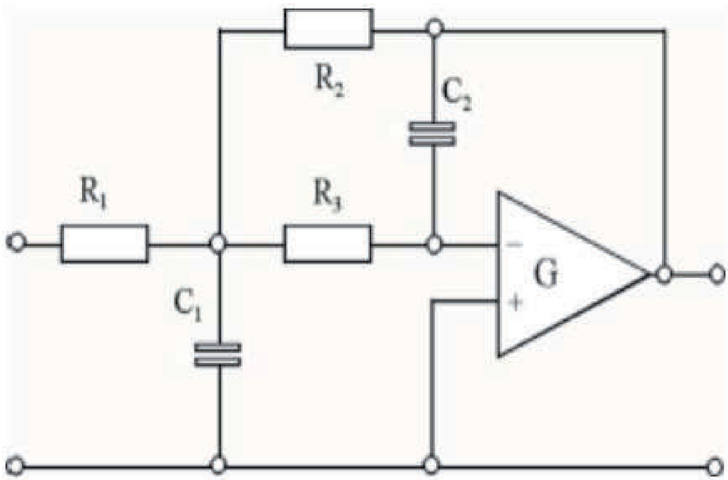

Figure 5: An active multi–pole UFL filter scheme. Selection of resistors R_1 and R_2, adjusts the gain of the filter. The cutoff frequency is set by R_1, R_3, C_1 and C_2 elements. UFL is usually trimmed by R_3.

detection, the FIFO mode is changed, freezing the data stored in the buffer. A decision to change the mode is made by the touchdown detection circuit, and performed by the trigger comparator. The FIFO, when full, contains 56 words corresponding to the pre–triggered state and 456 words corresponding to the post–triggered interval. Then the data is read together with the current onboard time by the SSP system processor.

A mechanism to freeze the FIFO data buffer is available for redundancy; the SSP processor using data from the ACC–I sensor can generate a trigger to freeze the FIFO.

5.7 Touchdown detection network

The force transducer is assumed to be the first part of the *Huygens Probe* which touches the ground on landing. The touchdown detection circuit starts the process of detection by observing the front–end signal and further converting it into a DC voltage (see Figure 6). A true RMS–to–DC converter calculates consecutive values of input signals and next accumulates results in an averaging capacitor C_{av}. The C_{av} is also modifying an error/settling time factor. A set of: R_{95} and C_{69}, as well as a two pole filter made of C_{68}, R_{95} and C_{64} reduces ripples of the buff–out voltage. The trigger level, set as $+V \cdot [(R^{*}/10k) + 1]$, is compared to the DC RMS component. When the trigger comparator sees an RMS level greater than the threshold, it generates the trigger signal freezing the FIFO full content of 512 words.

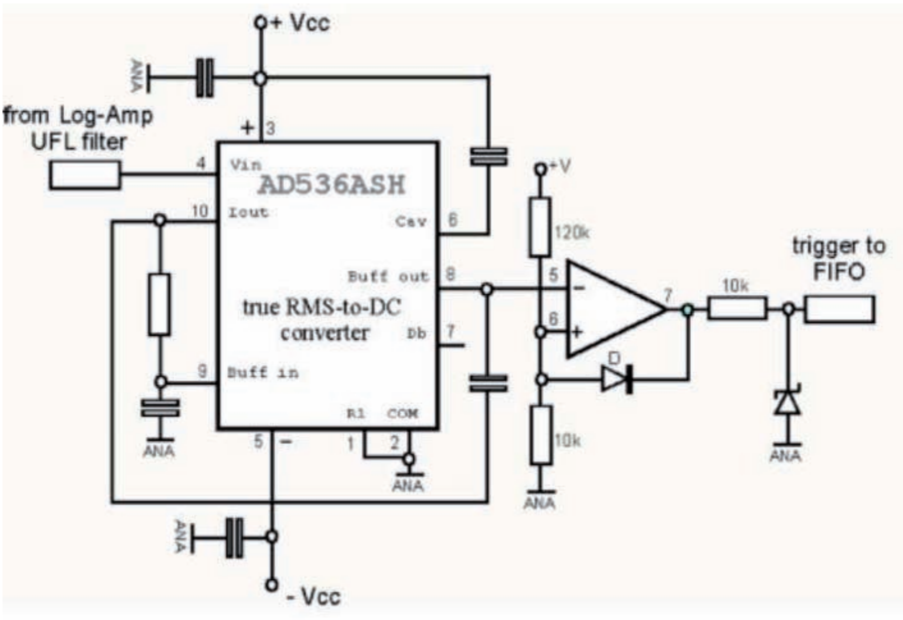

Figure 6: True RMS–to–DC converter precedes a trigger generator.

6 In–flight test facilities

The onboard electronics provides three different functions: science data collection, health checking, and in–flight testing. All these operations are coordinated by the SSP processor. The science operations are active mainly in final phases of the descent and landing, but all functions are useful for system diagnosis in preceding phases.

The ACC–E electronics self test function is used for health checking of the transducer, and to provide a monitor for sensor calibration. For that purpose the transducer has two sensing electrodes, one for final sensing the the touch down, and another one, which may serve sensing but also stimulating a transducer response artificially with the stimulus generated by the control system. The control system contains a shared signal generator for those purposes. The system provides control of the ACC–E transducer by stimulating its responses and the charge amplifier health by feeding it with an artificial signal, as well as feeding the signal to the ACC–I, TIL and PER instruments and forcing their proper responses. The health check sequence includes all necessary reference sources, provided by a number of precise voltage references $U_{REF} = 4.5$ V to compare their long–term stability. It is obvious that references are used also for the science operation. The health check sequence includes the power supply lines status after the power is switched on. It also includes several environmental temperature readings. The penetrometer sensor's ambient temperature monitoring is crucial during the first phase of the *Huygens Probe* entry to the atmosphere. This temperature sensor is a saturated transistor junction selected for wide range, from cryogenic to room and higher temperatures.

7 Conclusions

The use of a piezoelectric transducer proved to be the proper choice for the ACC–E instrument. The alternative choice, an accelerometer, was considered as too complex for the required control system and data handling. The electronic system was built as simple as possible for the sake of saving power consumption and maximizing reliability. Space–qualified electronic components available in 1992 did not allow more extensive signal processing and transmission.

Acknowledgements

ZJK acknowledges supports from the *Unit for Space Sciences* of the University of Kent at Canterbury, Kent (UK), from the *Electronics Design Group* of the Space Systems Division at Rutherford Appleton Laboratory, Didcot, Chilton (UK), and from the *Space Research Centre* of the Polish Academy of Sciences, Warsaw, Poland. ZJK also acknowledges his two–year hosting by the SSP team. ZJK thanks to Bill Duell for providing some plots used in this paper.

8 Appendix

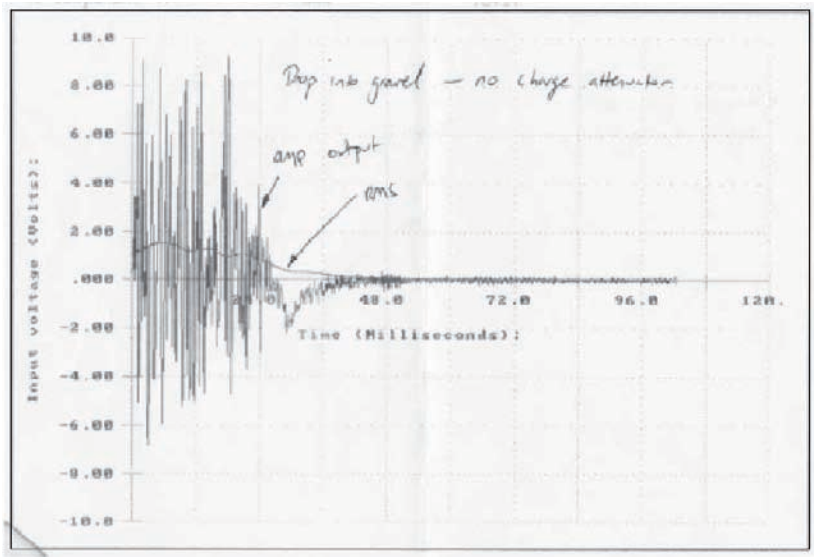

Figure 7: The plots shown above represent the penetrometer pylon dropped into gravel. This test is dated on April 7 1993. The sharp and of higher magnitude plot expresses bipolar output voltage of an amplifier used for the test. It is marked as "amp output". The signal generated under test conditions by the penetrometer sensor is fully linear. No logarithmic conversion has been used to prepare the sensor signal, and no charge attenuator was applied to protect the amplifier's input. An RMS–to–DC converter has been added to the test electronics in order to show its actual output signal. The smooth plot, marked "RMS", expresses the voltage at the output of the applied RMS circuit.

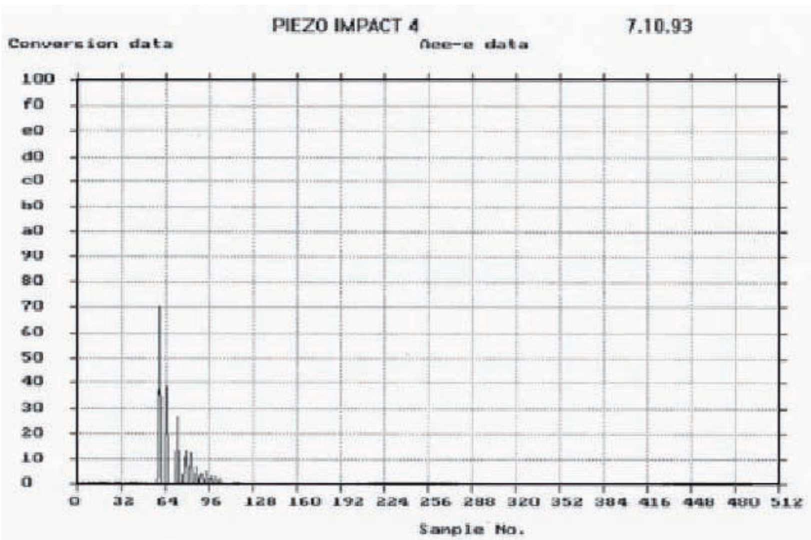

Figure 8: The impact test data measured by the ACC–E system tested in the laboratory on October 1993. The system contains: the sensor penetrating a sandy soil, the front–end electronics with the charge divider, the pseudo–logarithmic amplifier, the UFL filter, the S/H, the ADC, the FIFO buffer, and the touchdown detection circuitry. Timing electronics has been synchronized with a digital oscillograph applied to the test and the 10kHz frequency clock has been used in the ACC–E control system. The trigger has been placed to buffer at sample # 56 , so the plot shows the buffer pre–triggered state in the first part (samples 1 – 56, 5.6 ms) followed by 456 post–triggered samples (45.6 ms). The shown data magnitude range is arbitrary.

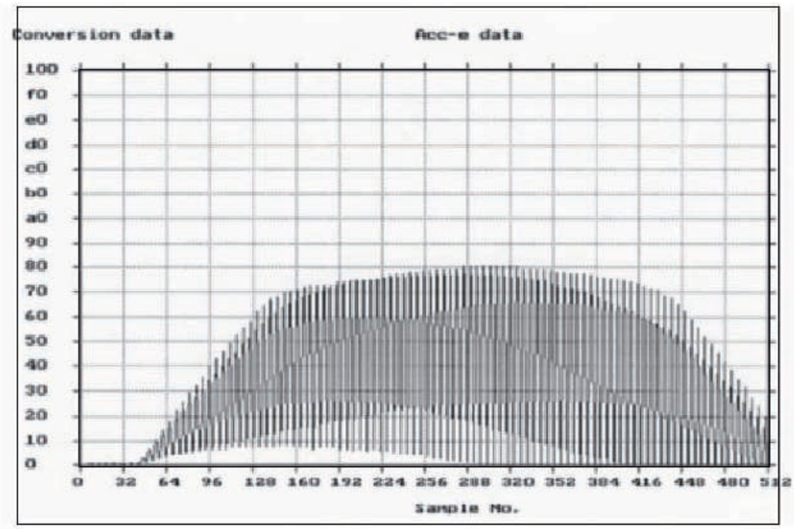

Figure 9: The stimulated impact test data measured by the ACC–E system. The test data has been measured by a simplified ACC–E system in October 1993. The force transducer was replaced by a waveform generator. A carrier sinusoidally modulated and next gated to the positive half wave lasting for about 50 ms has been supplied to the system's front–end electronics. The charge divider, the pseudo–logarithmic amplifier, the UFL filter, the S/H, the ADC, the FIFO buffer and the touchdown detection circuitry were added to the testing system, as well as the timing control electronics. The last one was synchronized with the digital oscillograph used for the test. The 10 MHz frequency clock has been used in the ACC–E control system and the oscillograph synchronization circuit. The ACC–E trigger has been placed to buffer at 48 preliminary sample, so the plot shows the buffer pre–triggered state (samples 1 – 48) and completing the buffer with the 466 post–triggered samples. The shown data magnitude range is arbitrary.

References

Encyclopaedia Britannica: Piezoelectric Devices, Vol. **XIV**, p. 451 (1977).

Lorenz R.D. et al.: An impact penetrometer for a landing spacecraft. *Meas. Sci. Technol.* **5**, 1033–1041 (1994).

Lorenz R.D. et al.: Titan surface mechanical properties from the SSP ACC–I record of the impact deceleration of the Huygens probe. *This volume* (2008).

Owen T.: Huygens rediscovers Titan. *Nature* **438**, 756–757 (2005).

Zarnecki J.C. et al.: A surface science package for the Huygens Titan probe. *Proc. Symposium on Titan*, Toulouse, France (1991).

Zarnecki J.C.: Surface science package for the Huygens Titan probe. *JBIS* **45**, 364–370 (1992).

Zarnecki J.C. et al.: A soft solid surface on Titan as revealed by the Huygens Surface Science Package. *Nature* **438**, 792–795 (2005).